

Evaporation and the Wetting of a Low-Energy Solid Surface

G. McHale,* S. M. Rowan, M. I. Newton, and M. K. Banerjee

Department of Chemistry and Physics, The Nottingham Trent University, Clifton Lane, Nottingham NG11 8NS, UK

Received: August 4, 1997; In Final Form: November 5, 1997

The evaporation of a small droplet of a volatile fluid from a solid surface differs according to whether the fluid wets the surface. When the initial contact angle is less than 90° , the evaporation initially proceeds with an accompanying decrease in the contact angle but no change in the contact radius. This stage of evaporation dominates the time scale and has previously been described by a diffusion model. However, when the initial contact angle is greater than 90° , it is the contact radius that decreases rather than the contact angle. In this work we report detailed measurements of the evaporation of drops of water from Teflon film. On deposition the contact angles rapidly relax from around 112° to 108° , which is the equilibrium value for droplets in a saturated vapor. The angle then remains constant for the majority of the evaporation time. Eventually the system changes to a mode of evaporation in which both contact angle and radius change simultaneously. The data are compared to an extension of the diffusion model, and this provides estimates of the diffusion coefficient. It is suggested that the constant contact angle observed during much of the evaporation is a result of a local saturation of the vapor in the region of the contact line.

Introduction

Birdi, Vu, and Winter¹ have shown that the rate of evaporation of a small droplet of fluid resting on a surface is influenced by the contact angle, θ , and hence the liquid–substrate interaction. They measured the change of weight of droplets of water on glass and concluded that for much of the time scale of the evaporation a linear evaporation rate holds. Subsequently, it was reported² that the evaporation of sessile drops of water on glass ($\theta = 41^\circ$) and *n*-octane on a Teflon surface was a stationary process with constant contact radius. The linearity of the evaporation rate for these systems of wetting liquids ($\theta < 90^\circ$) can be contrasted with the nonlinearity observed for water on Teflon ($\theta = 108^\circ$) and *n*-octane on Teflon. For nonwetting liquids with $\theta > 90^\circ$ a constant contact angle with a decreasing contact radius is observed which contrasts sharply with the wetting case of a constant contact radius and decreasing contact angle. One difficulty with these reports is that no precise measurements of geometrical parameters were obtained. Shanahan and Bourges³ also considered the evaporation of droplets of water from smooth polyethylene and both smooth and rough epoxy resin surfaces; these are all systems with $\theta < 90^\circ$. They obtained direct measurements of the change of drop height, contact angle, and contact radius with time. The evaporation was found to consist of several distinct stages, and in particular they identified a dominant stage of the evaporation that corresponded to the stationary contact radius mode of evaporation.

In two separate studies^{4,5} we presented detailed measurements of the change in contact angle with time for water on poly(methyl methacrylate) and for three alcohols resting on Teflon. A detailed theoretical model based on a diffusion model suggested by Birdi et al.¹ was given,⁴ and this was shown to be an adequate description of the observed changes in various geometrical parameters. However, all the systems previously studied with detailed observation of geometrical changes in time correspond to the wetting liquid case with $\theta < 90^\circ$. The aim of this article is to provide detailed measurements of geometrical

parameters for evaporation of sessile drops in a nonwetting system ($\theta > 90^\circ$). The changes in the contact radius are compared with an extension of the previously published diffusion model, and the diffusion coefficient is estimated. An explanation of the constant contact angle is proposed, and this also explains why the value observed should be the same as that measured for water on PTFE in a saturated vapor atmosphere.⁶

Experimental Details

A system of water on Teflon film was chosen for the study because this provided an initial contact angle larger than 90° . This surface is also sufficiently reflective to enable an optical profile of a droplet and its reflection to be obtained. Small drops of triply distilled water were deposited from a syringe onto the surface, which was used as received from du Pont. The evolution in the profile of the droplet was then recorded onto videotape operating at 25 frames/s. Subsequently, images were transferred onto a personal computer using a capture card working at a resolution of 680×460 pixels. Digital image analysis was performed using a simple thresholding routine to obtain the profile. A circular cap shape was then fitted to the obtained profile, and the contact angle, θ , contact radius, r_0 , circular radius, R , and the maximum height, h_0 , of the spherical cap above the substrate were extracted. In principle, gravity can be ignored, and a droplet can be expected to adopt a spherical cap shape if the radius is much less than a capillary length which is given by $\kappa^{-1} = (\gamma_{LV}/\rho g)^{1/2}$, where γ_{LV} is the liquid–vapor surface tension, ρ is the density of water, and g is the acceleration due to gravity. The drops in this study have initial spherical radii of 0.447, 0.567, 0.488, 0.541, and 0.646 mm. All experiments were conducted at a temperature of 21°C , and the relative humidity was 53% when the first two evaporation sequences were recorded and was 44% when the latter three were recorded. All the droplets have radii larger than 10% of the capillary length $\kappa^{-1} = 2.8$ mm of water, and so gravitational flattening may occur. The assumption of a

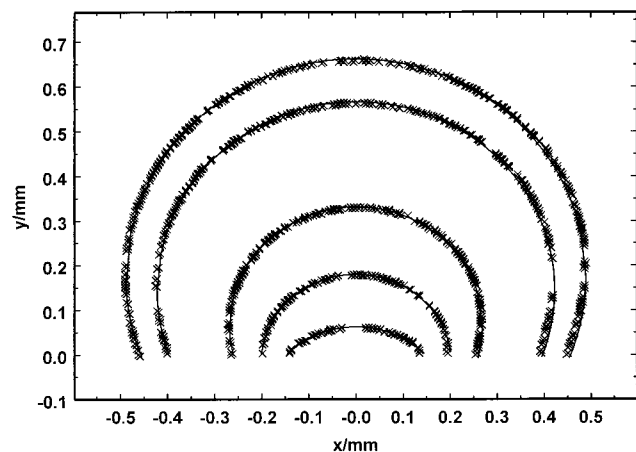


Figure 1. Profile of a droplet of $R = 0.488$ mm can be fitted by a spherical cap shape during the course of its evaporation; the times are 0, 175, 475, 595, and 655 s.

circular cross-sectional profile can therefore only be justified by reference to the accuracy of the fit although we would expect any distortion from a spherical cap shape to have only a marginal effect. The importance of such gravitational flattening for the wetting system has been considered by Erbil and Meric.⁷

Results

In Figure 1 we show a sequence of profiles, and the circular fits, as a droplet (initial circular radius of $R = 0.488$ mm) evaporates. The accuracy of the circular cap assumption appears to be good. The points plotted for any one profile are not uniformly spaced because only points where a change in direction occurs are indicated. It is difficult to identify any significant flattening due to gravitational influences. Such flattening would have to be larger than a few percent to be significant given the tolerance ($\pm 2\%$) in the calibration of the aspect ratio of the optical system. Immediately after deposition, a contact angle of 112° is observed which then relaxes within 200 s to a constant angle of 108° . This initial change in contact angle occurs equally on both sides of the droplet and is not accompanied by any change in the constant contact radius. Once the contact angle relaxes to 108° the contact radius begins to reduce systematically. After approximately 600 s the previously constant contact angle begins to fall rapidly. This is accompanied by an increasing rate of reduction of the contact radius with the final stage of evaporation being completed rapidly. This sequence of changes in the contact angle and radius is shown in Figure 2, and this diagram also emphasizes the extent to which the evaporation corresponds to a constant contact angle regime.

Figure 2 compares the changes in contact angle and contact radius for two droplets with initial spherical radii of $R = 0.488$ mm and $R = 0.646$ mm. After the constant contact angle mode ends, the data for both drops become more scattered with a steeper slope in the contact radius–time dependence evident after 600 and 1000 s, respectively. This change in slope may also be accompanied by a knee in the contact angle data at around 70° – 80° ; such a feature is seen in all our other data. However, the accuracy of the profile measurements is less as the contact angle approaches 90° . First, at a purely technical level it is more difficult to identify the baseline separating the droplet from its reflection. Second, the top of the droplet begins to lose its sharpness, and the contrast between the droplet and the background is reduced, leading to more uncertainty within the thresholding process. By stretching the contrast it is possible

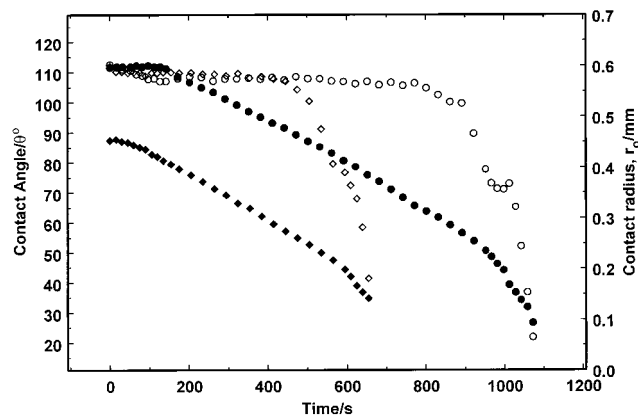


Figure 2. Contact angles (open circles and diamonds) for drops of $R = 0.488$ mm and $R = 0.646$ mm rapidly relax after deposition to a quasi-static value of around 108° . The corresponding changes in contact radius are shown by the solid symbols.

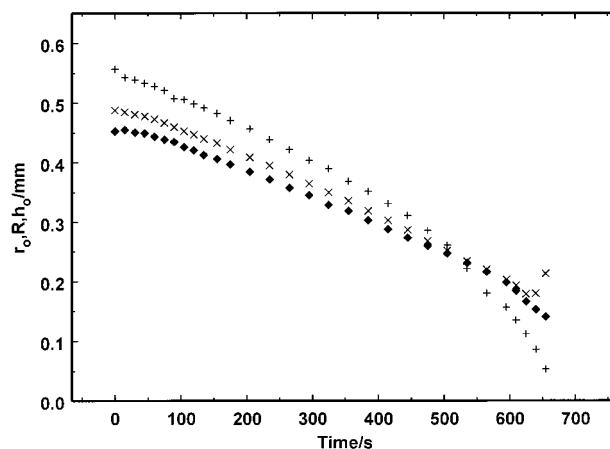


Figure 3. Contact radius (diamonds), spherical radius (crosses), and height (pluses) of the drop with $R = 0.488$ mm decrease steadily during the time the contact angle is constant.

on some images to qualitatively identify vapor leaving the top of a droplet. This vapor results in a less distinct upper edge to the image, and there is a danger of the profile being seen as artificially elliptical. However, it is possible to fit a circular cap shape to a partial profile, not including the upper edge, and this can be used to verify the fit to the full profile. Once the contact angle falls below 90° the small residual volume of the droplet decreases the accuracy of the measurements. The changes in spherical radius and height that accompany the reducing contact radius in the evaporation of the droplet shown in Figure 1 are presented in Figure 3; similar time dependencies are observed for all drops studied.

Discussion

For a small drop of fluid with the contact radius much less than the capillary length gravitational flattening of the droplet shape can be neglected. A spherical cap shape is adopted by the fluid, and this can be specified by its volume, V , and any two other parameters chosen from the contact radius, r_0 , spherical radius, R , contact angle, and droplet height, h_0 . The relationships between these variables are

$$r_0 = R \sin \theta \quad \text{and} \quad R = (3V/\pi\beta)^{1/3} \quad (1)$$

where

$$\beta = 2 - 3 \cos \theta + \cos^3 \theta \quad (2)$$

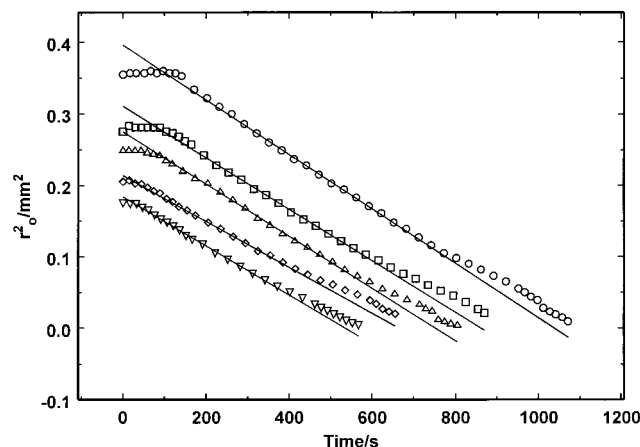


Figure 4. Linearity of r_0^2 during the constant contact angle period for drops of initial sizes $R = 0.646$ (circles), 0.567 (squares), 0.541 (upward triangles), 0.488 (diamonds), and 0.447 mm (downward triangles) is shown by the straight lines. The slopes are 3.82×10^{-10} , 3.60×10^{-10} , 3.65×10^{-10} , 3.23×10^{-10} , and $3.44 \times 10^{-10} \text{ m}^2 \text{ s}^{-1}$.

and V is the volume of fluid. The evaporation rate is taken to be due to diffusion through the liquid–vapor interface,

$$\frac{dV}{dt} = -\frac{D}{\rho} \int \nabla C \cdot dS \quad (3)$$

where D is the diffusion coefficient of the vapor and ρ is the density of water. Assuming the concentration gradient to be radially outward and equal to $(c_\infty - c_0)/R$, where c_0 and c_∞ are the concentrations of the vapor at the droplet–vapor interface and far removed from the interface, the evaporation rate can be expressed as

$$dV/dt = -\lambda h_0 \quad (4)$$

where $\lambda = 2\pi D(c_\infty - c_0)/\rho$. In our earlier work, we solved this equation for the experimentally observed case of relatively slow changes in the contact radius compared to the contact angle. The present data for a nonwetting data suggest that the contact angle is the slow variable compared to the contact radius. Equation 4 then reduces to

$$r_0 \frac{dr_0}{dt} = -\frac{\lambda \sin^2 \theta}{\pi(1 - \cos \theta)(2 + \cos \theta)} \quad (5)$$

and can be solved to give

$$r_0^2 = r_i^2 - \frac{2\lambda t \sin^2 \theta}{\pi(1 - \cos \theta)(2 + \cos \theta)} \quad (6)$$

where r_i is a constant of integration.

The time dependence of r_0^2 is shown in Figure 4 for all five sets of results. The solid lines are fits to each data set using the period in which the contact angle was constant at around 108° . Over this range, the quality of each fit is good, although the curvature in r_0 with time is sufficiently small that it can also be reasonably fitted by a straight line. To provide added confidence in the accuracy of an r_0^2 dependence, we have estimated the diffusion coefficients from the slopes, m , of the data in Figure 4 using $D = mp/4(c_\infty - c_0)f(\theta)$ where $f(\theta) = \sin^2 \theta/(1 - \cos \theta)(2 + \cos \theta)$. For example, for the droplet with initial contact radius of 0.488 mm, the slope is $3.44 \times 10^{-4} \text{ mm}^2 \text{ s}^{-1}$, and $\theta = 108^\circ$. The relative humidity of 44% and temperature of 21°C give⁸ $(c_\infty - c_0) = 10.11 \text{ g m}^{-3}$, and so the diffusion coefficient is $D = 1.96 \times 10^{-5} \text{ m}^2 \text{ s}^{-1}$. The

estimates of D for the data in Figure 4 lie between 2.61×10^{-5} and $1.96 \times 10^{-5} \text{ m}^2 \text{ s}^{-1}$ with an average value of $2.32 \times 10^{-5} \text{ m}^2 \text{ s}^{-1}$. This compares favorably with the value obtained from the CRC Handbook⁸ of 2.39×10^{-5} for water vapor into air at 8°C which corrected for 21°C using a $T^{3/2}$ temperature dependence gives $2.56 \times 10^{-5} \text{ m}^2 \text{ s}^{-1}$.

The diffusion model appears to describe the relationships between the various geometrical factors and time, but it is semiempirical and requires an assumption about which variables change slowly. In the wetting case, with an initial contact angle of less than 90° , the evaporation is dominated by a stage in which the contact radius hardly changes. This contrasts sharply with the nonwetting case where the dominant stage has a quasi-static contact angle. Moreover, the value of this angle ($\approx 108^\circ$) is precisely that which has been reported from a water drop on Teflon surface in a water vapor saturated atmosphere.⁶ The origin of this appears to be the assumption of a concentration gradient directed radially outward and equal to $(c_\infty - c_0)/R$. Close to the solid surface this assumption will fail. When the contact angle is greater than 90° , the space between the solid–vapor interface and the liquid–vapor interface is constricted, and a rapid saturation of vapor near the contact line is likely to occur. The three interfacial forces at the contact line are γ_{LV} , γ_{SV} , and γ_{SL} where the subscript V refers to water saturated vapor. These can be balanced to give the usual Young’s law for the contact angle, $\cos \theta = (\gamma_{SV} - \gamma_{SL})/\gamma_{LV}$. As the evaporation proceeds, the volume of the drop reduces, but the vapor in the restricted space near to the contact line remains saturated. This is because of the vapor created as the contact line retracts and also because of the obtuse shape of the droplet which hinders the flow of air near the contact line. The force balance argument is therefore unchanged, and the contact angle remains constant so that the reduced liquid volume results only in a reduced contact radius. If this picture is correct, the diffusion model overestimates the amount of liquid–vapor surface through which diffusion occurs. For example, assuming a worst case in which diffusion occurs only across the upper half-sphere of the surface, eq 6 would become

$$r_0^2 = r_i^2 - \frac{2\lambda t \sin^2 \theta}{\pi(2 + \cos \theta)} \quad (7)$$

The basic time dependence of r_0^2 would therefore be unaltered, and the main consequence would be to change the estimated diffusion coefficient by, at most, a factor of 1.31. It seems reasonable to suppose that as the drop size reduces, air is able to circulate closer to the contact line until eventually the local saturation is removed. This would then alter the force balance, and the contact angle would begin to change. In contrast, if the system is wetting, the initial contact angle is less than 90° , and the air flow around the contact line will be easier. This will prevent a local saturated vapor being created, the constant force balance argument will not occur, and there is no reason to expect a constant contact angle mode of evaporation. A nonwetting system with an initial contact angle larger than 90° can therefore be expected to behave quite differently from a wetting system.

Several other physical effects, such as surface roughness and evaporative cooling, may be important in the evaporation of drops from solid surfaces. Extrand and Kumagai⁹ have examined the influence of surface roughness on contact angle hysteresis for water drops on inclined PTFE surfaces. They reported that the drops moved with a slip-stick motion and that this was most pronounced on the rough PTFE. In our case, the motion of the receding contact line was smooth during the

constant contact angle phase of evaporation. However, a slip-stick motion due to surface roughness may be an explanation for the apparent knee in the contact angle data at around 70–80°. In the evaporation from a wetting surface, for which we have suggested a locally saturated vapor is not generated, roughness could play an immediate role in pinning the contact line. This may then ensure that the initial stage corresponds to a constant contact radius mode of evaporation. Another major influence may be the inevitable cooling of the droplet that will accompany the evaporation. Such a cooling is likely to preferentially cool the apex of the droplet compared to the contact line. This would lead to surface tension gradients and hence Marangoni forces. Rymkiewicz and Zapacowicz¹⁰ have suggested such gradients can cause the convective currents and contact line instabilities they observed in the evaporation of droplets from a heated surface. This effect may also contribute to the increasing scatter in our data as the constant contact angle mode of evaporation ends. Such a mechanism could also cause increasing scatter in the data at the end of the constant contact radius mode of evaporation for drops on a wetting surface.⁵

Conclusion

The changing profile of small sessile droplets of water evaporating from a PTFE surface has been studied. The time scale is dominated by a regime with the contact angle constant at the saturated vapor equilibrium value of 108°. A model based on diffusion across the liquid–vapor interface has been developed, and this predicts a linear dependence on time for the square of the contact radius. Data for droplets with initial spherical radii of between 0.447 and 0.646 mm are consistent

with the model and allow the diffusion constant to be estimated. It is suggested that a local saturated vapor is created near the contact line, and this explains why the contact angle is constant at 108°. Moreover, the saturated vapor hypothesis also explains why the evaporation of droplets in nonwetting systems should differ from that of wetting systems.

Acknowledgment. Image processing was performed using UTHSCSA ImageTool program (developed at the University of Texas Health Science Center at San Antonio, Texas, and available from the Internet by anonymous FTP from maxrad6.uthscsa.edu). One of the authors (G.M.) would like to acknowledge Dr. H. Y. Erbil for discussions on the topic of this article.

References and Notes

- (1) Birdi, K. S.; Vu, D. T.; Winter, A. *J. Phys. Chem.* **1989**, *93*, 3702.
- (2) Birdi, K. S.; Vu, D. T. *J. Adhes. Sci. Technol.* **1993**, *7*, 485.
- (3) Shanahan, M. E. R.; Bourges, C. *Int. J. Adhes. Adhes.* **1994**, *14*, 201.
- (4) Rowan, S. M.; McHale, G.; Newton, M. I. *J. Phys. Chem.* **1995**, *99*, 13268.
- (5) Rowan, S. M.; McHale, G.; Newton, M. I.; Toorneman, M. *J. Phys. Chem. B* **1997**, *101*, 1265.
- (6) Yekta-Fard, M.; Ponter, A. B. *J. Colloid Interface Sci.* **1988**, *126*, 134.
- (7) Erbil, H. Y.; Meric, R. A. *J. Phys. Chem. B*, in press.
- (8) Weast, R. C.; Astle, M. J. *CRC Handbook of Chemistry and Physics*, 62nd ed.; CRC Press: Boca Raton, FL, 1981–1982.
- (9) Extrand, C. W.; Kumagai, Y. *J. Colloid Interface Sci.* **1995**, *170*, 515.
- (10) Rymkiewicz, J.; Zapacowicz, Z. *Int. Commun. Heat Mass Transfer* **1993**, *20*, 687.